# Combined Impacts of ENSO and MJO on the 2015 Growing Season Drought on the Canadian Prairies

Zhenhua Li[1,2], Yanping Li[1], Barrie Bonsal[3], Alan H. Manson[2], Lucia Scaff[1]

[1]Global Institute for Water Security, University of Saskatchewan, Saskatoon, Saskatchewan, Canada S7N3H5

[2]Institute of Space and Atmospheric Studies, University of Saskatchewan, Saskatoon, Saskatchewan, Canada

[3]National Hydrology Research Center, Environment and Climate Change Canada, Saskatoon, SK, Canada

*Correspondence to*: Dr. Yanping Li (yanping.li@usask.ca); Dr. Zhenhua Li (zhenhua.li@usask.ca)

**Abstract**

Warm-season precipitation on the Canadian Prairies plays a crucial role in agricultural production. This research investigates how the early summer 2015 drought across the Canadian Prairies is related to the tropical Pacific forcing. The significant deficit of precipitation in May and June 2015 coincided with a warm phase of El Nino-Southern Oscillation (ENSO) and a negative phase of Madden-Julian Oscillation (MJO)-4 index, which favour a positive geopotential height anomaly in western Canada. Our further investigation during the instrumental record (1979-2016) shows that warm-season precipitation in the Canadian Prairies and the corresponding atmospheric circulation anomalies over western Canada teleconnected with the lower boundary conditions in the tropical western Pacific. Our results indicate that MJO can play a crucial role in determining the summer precipitation anomaly in the western Canadian Prairies when the equatorial central Pacific is warmer than normal (NINO4 > 0) and MJO is more active. This teleconnection is due to the propagation of a stationary Rossby wave that is generated in the MJO-4 index region. When the tropical convection around MJO-4 index region (western tropical Pacific, centred over 140°E) is more active than normal (NINO4 > 0), Rossby wave trains originate from the western Pacific with wavenumbers determined by the background mean wind and meridional absolute vorticity gradient. Under warm NINO4 conditions waves are generated with smaller wavenumbers compared to cold NINO4 conditions. These waves under warm NINO4 can propagate into the midlatitudes over North America causing a persistent anomalous ridge in the upper level over western Canada, which favours dry conditions over the region.

# 1 Introduction

The Canadian Prairies depend on summer precipitation especially during the early to mid-growing season (May through August) when the majority of annual precipitation normally occurs (e.g., Bonsal *et al*. 1993). High natural variability in growing season precipitation causes periodic occurrences of extreme precipitation (Li et al. 2017; Liu et al. 2016) and droughts that are often associated with reduced agriculture yields, low streamflow, and increased occurrence of forest fires (Wheaton et al. 2005, Bonsal and Regier 2007). Drought events with great environmental and economic impacts on the Canadian Prairies have occurred in 1961, 1988, 2001-2002, and as recent as 2015 (Dey 1982, Liu *et al*. 2004, Bonsal *et al*. 1999, Wheaton *et al*. 2005, Shabbar *et al*. 2011, Bonsal *et al*. 2013, Szeto *et al*. 2016). The sub-seasonal forecast of precipitation for the growing season is crucial for the agriculture, water resource management, and the economy of the region. Therefore, an investigation into the causes of inter-annual variability in the growing season precipitation of the Canadian Prairie is needed.

Low precipitation and extended dry periods on the Canadian Prairies are often associated with an upper-level ridge and a persistent high pressure centred over the region (Dey 1982, Liu *et al*. 2004). These prolonged atmospheric anomalies often concurred with abnormal boundary layer conditions such as a large-scale sea surface temperature (SST) anomalies in the Pacific Ocean (Shabbar and Skinner 2004). Large-scale oscillation in the SST anomalies in the Pacific Ocean, namely El Nino, and the Pacific Decadal Oscillation (PDO), can affect the hydroclimatic pattern in summer over North America, although the strongest impacts of these boundary conditions occur during the boreal winter. Inter-annual variability such as El Nino-Southern Oscillation (ENSO) is linked with extended droughts in the Prairies (Bonsal *et al*. 1999, Shabbar and Skinner 2004). Interdecadal oscillations such as the PDO, and the Atlantic Multi-decadal Oscillation (AMO) also affect the seasonal temperature and precipitation in the Canadian Prairies (Shabbar *et al*. 2011).

ENSO's relationship with the Canadian Prairies' precipitation has been studied extensively. Previous investigations (e.g., Shabbar *et al*. (2011)) have found that El Nino events are associated with a summer moisture deficit in western Canada while La Nina events cause an abundance of moisture in far western Canada (British Columbia and Yukon). However, they also noted that although tropical SST variability accounted for some aspects of the large-scale circulation anomalies that influence the Canadian Prairies meteorological drought, a consistent and clear-cut relationship was not found. The warm phase of ENSO often favours drought in this region, especially during the growing season after the mature phase of El Nino (Bonsal and Lawford 1999, Shabbar and Skinner 2004). The positive North Pacific Mode (NPM, Hartmann *et al.* 2015) like North Pacific SST anomaly pattern often follows a matured El Nino, and the accompanying atmospheric ridging leads to extended dry spells over the Prairies during the growing season (Bonsal and Lawford 1999). Furthermore, in association with the recent North Pacific SST anomaly from 2013 to 2014, researchers have attributed the precipitation deficit in California during 2013 to the anomalous upper-level ridge over western North America (Wang *et al*. 2014, Szeto *et al*. 2016).

The aforementioned SST variations mostly vary on inter-annual and decadal scales. Another important factor that affects the weather patterns in North America is the Madden-Julian Oscillation (MJO), an intra-seasonal (40-90 days) oscillation in convection and precipitation pattern over the Tropics (Madden and Julian 1971, Zhang 2005, Riddle *et al.* 2013, Carbone and Li 2015). MJO is a coupled atmosphere-ocean oscillation involving convection and large-scale equatorial waves, which produces an eastward propagation of tropical convection anomaly (Madden and Julian 1971). The MJO affects the winter temperature and precipitation in North America and Europe through its impact on moisture transport associated with the "Pineapple Express" and its effects on the North Atlantic Oscillation and stratospheric polar vortex (Cassou 2008, Garfinkel *et al.* 2012, Rodney *et al*. 2013). MJO is also connected to the summer precipitation anomalies in the Southwest United States (Lorenz

and Hartmann 2006). During the warm season, MJO's impact on the Canadian Prairies' precipitation has not been thoroughly investigated as MJO's amplitude is weak during spring and early summer. The amplitude of MJO in spring and early summer is related to the inter-annual variation of tropical SST, especially the SST in central Pacific (Hendon *et al*. 2007, Marshall *et al*. 2016). MJO in terms of the Real-time Multivariate MJO index (RMM, Wheeler and Hendon 2004), was extremely strong in the early spring of 2015 with a positive PDO-like SST anomaly in the central Pacific and at the same time, El Nino started to strengthen.

MJO activities in the western Pacific under the modulation of inter-annual SST variability have the potential to act together with ENSO and impact mid-tropospheric circulation over western Canada and thus, warm season precipitation over the Canadian Prairies. The goal of this study is to demonstrate that MJO has contributed to the 2015 growing season drought in the Canadian Prairies through the propagation of stationary Rossby wave. Subsequently, further investigations are carried out to determine if similar relationships exist in association with other summer extreme precipitation events during instrumental record (1979-2016). Section 2 provides the datasets and methodology used in this paper while section 3 presents the analysis of the upper-level circulation anomaly and SST pattern associated with the 2015 drought. This is followed by the examination of the effects of central Pacific SST anomalies and MJO on the summer precipitation in the Canadian Prairies. The mechanism by which MJO affects summer precipitation when equatorial central Pacific SST is warmer than normal is discussed in section 4 followed by the summary and concluding remarks in section 5.

# 2 Data and Methodology

Multiple observation and reanalysis datasets are used to investigate the circulation anomalies associated with the Canadian Prairies' growing season (May-August) precipitation. The observed precipitation is taken from the Climate Prediction Center (CPC) Merged Analysis of Precipitation

(CMAP) dataset (Xie and Arkin 1997). Geopotential height fields from the National Center for Environmental Predictions (NCEP) Reanalysis (Kalnay *et al.* 1996) and the European Center for Medium-Range Weather Forecast (ECMWF)'s ERA-Interim reanalysis (Dee *et al.* 2011) are used to analyze the mid- and upper-level (500 hPa and 200 hPa) atmospheric circulation patterns.

To represent the central Pacific SST anomaly, NINO4 SST index (Rayner *et al*. 2003) from CPC of National Oceanic and Atmospheric Administration (NOAA) is used since the NINO4 region is near the central Pacific and spans over the dateline (5°S-5°N, 160°E-150°W). Multivariate ENSO Index (MEI) data are retrieved from NOAA's Climate Data Center (CDC) website and is used to determine the ENSO phase (Wolter 1987, Wolter and Timlin 1993). In particular, El Nino condition is defined when the monthly mean index of MEI is larger than 0.5 (Andrews *et al*. 2004).

The Real-time Multivariate MJO series (RMM1 and RMM2) developed by Wheeler and Hendon (2004) are used to identify periods of strong MJO activity as the MJO amplitudes are directly calculated by the square root of RMM1 + RMM2. For MJO intensities over the investigated regions, we used the monthly averaged pentad MJO indices from NOAA CPC's MJO index (Xue *et al*. 2002), which have 10 indices representing locations around the globe. The CPC's MJO index is based on Extended Empirical Orthogonal Function (EEOF) analysis on pentad velocity potential at 200 hPa. Ten MJO indices on a daily scale are constructed by projecting the daily (0000 UTC) velocity potential anomalies at 200 hPa (CHI200) onto the ten time-lagged patterns of the first EEOF of pentad CHI200 anomalies (Xue *et al*. 2002). Negative values of ten MJO indices correspond to enhanced convection in the 10 regions centred on 20°E, 70°E, 80°E, 100°E, 120°E, 140°E, 160°E, 120°W, 40°W and 10°W in the tropics. MJO indices usually vary between -2 to 2 with negative values indicating above average convective activities in the corresponding region. Because boreal summer usually corresponds to a period of a weaker amplitude of MJO than the winter, we chose the monthly mean value of -0.3 as the criterion of strong convection which is connected to MJO as the index generally vary between -1 and 1. An MJO-4 index (centred on

140°E) of less than -0.3 was considered a relatively strong convection in the western Pacific, which has been found to be a source region of stationary Rossby waves (Simmons 1980). SST observations include Extended Reconstructed Sea Surface Temperature (ERSST) v4 (Huang *et al.* 2015). Outward Longwave Radiation (OLR) data from NOAA Interpolated Outgoing Longwave Radiation are used to derive the composite of anomalies of OLR for a certain phase of MJO.

Our study focuses on the growing season precipitation in the provinces of Alberta and Saskatchewan in the Canadian Prairies, where the largest deficits were observed in 2015. Specifically, the regional mean precipitation over 115°-102.5°W, 50°-57.5°N is used (boxed area in Fig. 1, top panel) to represent the Canadian Prairies east of the Rocky Mountains and south of the boreal forest. The chosen region also covers most of the arable land in the Canadian Prairies. Considering the unique MJO-4 and NINO4 indices for 2015, the relationship between the Prairies' warm season (May-August) precipitation with MJO-4 and ENSO during the instrumental records are investigated using correlation and regression. Though the dry months of the 2015 growing season are May and June when MJO-4 was in negative phase, we want to study the statistical relationship between MJO-4 and the Prairies' precipitation in the whole period of growing season (May-August). The possible mechanism behind the correlation between MJO-4 and the Prairies' warm season precipitation under El Nino condition is further investigated by analyzing the upper-level circulation associated with convection in the tropical Pacific and stationary Rossby waves in mid-latitudes.

# 3 Results

## 3.1 The 2015 Summer Drought

Almost all of western Canada including British Columbia, the southern Northwest Territories, Alberta, and Saskatchewan had negative precipitation anomalies during May and June 2015. The top plot in Fig. 1 shows the precipitation anomaly in percentage relative to the climatology (1981-2010 long-term mean) in Canada during May and June 2015. The bottom plot in Fig. 1 presents the monthly precipitation anomaly averaged over the region encompassed by the dash lines (top panel in Fig. 1). The average annual cycle of the regional precipitation has a dry period between February and May and June has the largest precipitation in all months. The May and June 2015 precipitation deficit was also accompanied by a relatively dry period from February to April [Fig.1 and Szeto *et al*. 2016], which added to the drought conditions.

The 500 hPa geopotential height (GHP) anomaly averaged in May and June are examined together with SST anomaly and ENSO, MJO-4 indices for 2014 and 2015. The 500 hPa GPH anomaly for May and June 2015 shows strong positive anomalies near Alaska and the British Columbia coast (Fig. 2), which is consistent with the findings for other episodes of growing season droughts (e.g., Dey 1982; Bonsal and Wheaton, 2005). Accompanying this anomalous ridge, are above normal SSTs in the northeast Pacific off the coast of North America and the central-eastern Pacific (Fig. 3). Both ENSO and the NPM are in positive phases that correspond to a warmer SST near the Pacific coast of North America, consistent with the positive GPH anomalies in western Canada and Alaska. The ridge in Alaska/Bering Straits and the one near British Columbia coast have been previously associated with El Nino and North Pacific SST anomaly such as NPM (Shabbar *et al.* 2011). The monthly mean anomalous ridge prevents storms from reaching the British Columbia coast and the Canadian Prairies causing extended dry spells. Therefore, the GPH anomaly in early growing season in 2015 is consistent with the

160 precipitation anomaly in these regions. The anomalous upper-level ridge in the Western United States
161 and Canada in 2014 and 2015 have also been associated with the developing El Nino and the other main
162 components of Pacific SST variation such as NPM by several recent studies (Hartmann *et al*. 2015, Lee
163 *et al*. 2015, Li *et al*. 2017).

164 The SST anomaly and the associated oscillations/modes, especially ENSO, show consistent
165 agreement with the observed GPH anomaly pattern. The average SST anomaly during the growing
166 season (May-June, July-August) of 2015 shows a persistent strong positive anomaly in the northeast and
167 eastern equatorial Pacific (Fig. 3), which corresponds to the warm phase of NPM and ENSO. SSTs in
168 the eastern tropical Pacific warmed increasingly since the end of 2014 and qualified as an El Nino in
169 early 2015. The NPM became positive in fall 2013, turned exceptionally strong in 2014 and persisted to
170 2015 (Hartmann 2015). The anomalous ridge is concurrent with strong SST anomalies in the tropical
171 Pacific and extratropical North Pacific. NPM, as the third EOF of Pacific SST (30°S-65°N), has also a
172 strong connection to the anomalous ridge in western North America and trough in the eastern US and
173 Canada in 2013-2014 winter (Hartmann 2015, Lee *et al.* 2015). During the ENSO-neutral condition in
174 2013 and 2014, the precursor of ENSO, the so-called "footprinting" mechanism is considered to cause
175 this anomalous ridge in western North America (Wang *et al.* 2014).

176 The variation of the Canadian Prairies' precipitation and its relationship with NINO4 and MJOs
177 are shown in Fig. 4. The time series of monthly RMM amplitude, NINO4 index, MJO-4 indices and the
178 Canadian Prairies' precipitation anomaly from January 2014 to December 2015 shows the atmospheric-
179 oceanic circulation indices for the drought in 2015. In May and June 2015, the western Pacific witnessed
180 a strong MJO-4 negative index, whereas in July the MJO-4 index became positive. This corresponds
181 well with the precipitation anomaly in Fig. 1. As shown in Fig. 3, El Nino continued to strengthen in
182 July and August 2015; while at the same time the MJO-4 index increased. The increase of the MJO-4
183 index indicated that the active convection associated with MJO moved away from the tropical western

Pacific region and propagated eastward into the central Pacific. Coincident with this change in MJO, the precipitation in the Canadian Prairies then returned to slightly above normal in July.

The good correspondence of MJO-4 and the negative precipitation anomaly suggests a link between MJO and Prairie precipitation during the growing season. Although El Nino and associated Northeast Pacific SST warm anomaly (i.e., NPM) in summer 2015 can be a contributing factor for the persistent upper-level ridge over the west coast of Canada (Shabbar *et al.* 2011), it cannot fully explain the drought condition in western Canada, as these SSTs do not guarantee a prolonged dry spell as shown by correlation analysis (Table 1). The negative MJO-4 index concurred with the negative anomaly of the Prairies' growing season precipitation in 2015, which prompts the investigation of their relationship with the instrumental records.

## 3.2 Instrumental record

El Nino and its associated North Pacific SST anomaly may contribute to extended dry spells in Canadian Prairies after the mature phase of El Nino (Bonsal *et al.* 1993) on an inter-annual time scale. ENSO, however, is not a strong intra-seasonal to seasonal predictor of Canadian Prairie summer precipitation. The lack of a strong correlation between the Prairies' precipitation and ENSO index can be caused by the fact that many factors can affect the Prairies' precipitation on a seasonal and sub-seasonal scale. Shabbar and Skinner (2004) showed the connection between the warm phase of ENSO and western Canadian drought through singular value decomposition analysis. However, they also found other modes of SST variation (e.g., the positive phase of PDO) can produce a wet condition in the Prairies. Here we present a new result showing that under warm central Pacific SST conditions (NINO4 > 0), a certain phase of MJO, which connected to the active convection in the tropical western

206 Pacific (Li and Carbone 2012), plays an important role in modulating the growing season precipitation
207 in the Canadian Prairies.

208 The correlation coefficients between the mean regional precipitation anomaly over Canadian
209 Prairies and MJO-4 indices and MEI from May to August are shown in Table 1. The correlation
210 between MEI alone and the precipitation anomalies is not significant. The correlation between MJO-4
211 and precipitation in the Prairies is 0.18 with a p-value of 0.023, which indicates that stronger tropical
212 convection in the equatorial region centred around 140ºE favours less precipitation in the Canadian
213 Prairies from May to August. When NINO4 is larger than 0, the correlation between MJO-4 and the
214 growing season precipitation is 0.33 with a p-value of 0.0015. Conversely, the correlation between
215 MJO-4 and Canadian Prairie precipitation is -0.01 when NINO4 < 0.

216 The scatter plot in Fig. 5 shows the distribution of monthly precipitation anomaly versus MJO-4
217 index and NINO4 index. Circled asterisk denotes a month with precipitation anomaly larger than 18
218 mm/month and the red (blue) circles denote a negative (positive) precipitation anomaly. The criterion
219 for precipitation anomaly to be emphasized by the circles is roughly one-third of the mean monthly
220 precipitation in the growing season. The size of the circle represents the magnitude of the monthly
221 precipitation anomalies with 6 mm/month interval. The bottom-right quadrant, indicated by shading,
222 shows that negative MJO-4 corresponds to many more dry months than wet months under NINO4 > 0
223 conditions. We noticed that some significant dry months are not in the shaded area, which corresponds
224 to the dry months occurring during La Nina or in the period after the mature phase of El Nino (Bonsal *et*
225 *al*. 1999). Summer drought in the Prairies can occur in both phases of ENSO or any other teleconnection
226 indices. For example, for the summer drought that happened in the Prairies from 1999 to 2005, the
227 large-scale anomalous patterns of SST first showed La Nina conditions and then became a weak El Nino
228 in the latter half of the period (Hanesiak *et al.* 2011). Bonsal and Wheaton (2005) showed that the
229 tropospheric atmospheric circulation patterns in 2001 and 2002 lacked the typical meridional flow in the

North Pacific and North America during the drought in western Canada. Their results show that the drought in 1999-2005 was related to the expansion of the continuous drought happened in the US to the north.

The impact of ENSO on the growing season precipitation over Canadian Prairies is investigated through Fig. 6. The box-percentile plot in Fig. 6 shows the distribution of monthly Canadian Prairies' precipitation anomalies from May to August along with different ENSO conditions. In general, under El Nino and neutral ENSO conditions, the precipitation anomalies are centred around 0, and there is no bias toward either end. Under La Nina condition, the mean precipitation has a positive bias. There are only 10 summer months under La Nina condition, whereas there are 71 months under El Nino and neutral conditions.

The distributions of precipitation anomalies versus MJO-4 index under different ENSO conditions are shown in Fig. 7. For NINO4 > 0, the precipitation anomaly has a negative tendency when MJO-4 < -0.3. With NINO4 < 0, there is no negative tendency for MJO-4 < -0.3. Therefore, Fig. 6 and 7 agrees with the significant correlation between precipitation and MJO-4 under NINO4 > 0, relative to ENSO in Table 1.

The correlation between MJO-4 and the Prairies' precipitation during the growing season leads us to investigate the underlying circulation anomalies. Fig. 8 presents the regressed stream function and wind field at 200 hPa in the mid-latitudes (north of 30°N) on the negative MJO-4 index from May to August under warm NINO4 SST condition (NINO4 > 0.5). In the tropics (10°S-20°N), during Northern Hemisphere summer, the OLR, velocity potential, and divergent wind vector are presented. Only regression patterns having p-values lower than 0.05 are plotted for OLR and velocity potential. The negative MJO-4 index corresponds to a negative anomaly in OLR, stronger convection and larger than average divergence at 200 hPa in the region centre around 150°E. The strong convection anomaly

centres around 150°E, 5°N with divergent wind extending well into the subtropics in the Northern Hemisphere. The positive GPH/stream function anomaly extended from Japan to central Pacific is associated with the enhanced convection and divergence in the upper troposphere over the western tropical-subtropical Pacific. A Rossby wave train linked to the OLR anomaly and strong divergence in the western Pacific propagate eastward into North America in the extratropics. To better demonstrate the propagation of the wave train, we conducted a ray tracing experiment of stationary Rossby wave following the nondivergent barotropic Rossby wave theory of Hoskins and Karoly (1981) and Hoskins and Ambrizzi (1993). Equation 1 describes the group velocity, which represents the propagation of wave activity. $C_{gx}$ and $C_{gy}$ are the group velocity components on zonal and meridional directions; $\overline{U}$ and $\overline{V}$ are the mean zonal and meridional winds; q is the mean absolute vorticity; *K*, *k*, *l* are the total wave number, zonal wavenumber, and meridional wavenumber, respectively. The ray path is integrated using a fourth-order Runge-Kutta method.

$$C_{gx} = \overline{U} + \frac{(k^2 - l^2)q_y - 2klq_x}{K^4}$$
$$C_{gy} = \overline{V} + \frac{(k^2 - l^2)q_x + 2klq_y}{K^4} \qquad \text{Equation 1}$$

Under the average conditions in May-August derived from ERA-Interim at 200 hPa with NINO4 > 0.5 or NINO4 < -0.5, we released rays with a total wavenumber matching with the mean flow at the extratropical location of the OLR anomaly (140°E-150°E, 25°N-30°N). For quasi-stationary waves, the wavenumber is determined by the basic zonal flow and background absolute vorticity gradient through the Rossby wave dispersion relation. For NINO4 >0.5 May-August condition, K =

4.14. With this total wavenumber and launching angle from 0- 60° relative to the zonal direction, Rossby wave rays (coloured by red, orange to blue according to their angle from 0° to 60°) released at 140°W, 20°N can propagate successfully to the western Canada for those with smaller launching angles (< 30°) as shown the bottom plot in Fig. 9. With NINO4<-0.5, the zonal wind in the source region is weaker, and the meridional gradient of absolute vorticity is stronger due to its relative further southern position to the subtropical jet. The total wavenumber for stationary Rossby waves is 6.2, determined by the mean May-August condition for NINO4 < -0.5. The waves with shorter wavelength tend to be evanescent near the source region as shown in the top plot in Fig. 9. However, there is no significant difference in ray-path under NINO4 < -0.5 condition compared to NINO4 > 0.5 if the source wavenumbers are set to the same value (results not shown). The changes in the mean conditions in the midlatitudes away from the source region from El Nino to La Nina are not sufficient to alter the propagation condition for quasi-stationary Rossby waves.

# 4 Discussion

Summer of 2015 is the first summer after the developing of El Nino during 2014-2015 winter. Though the upper-level GPH pattern, seen in summer 2015, can be attributed to the SST modes in the Pacific, namely ENSO and NPM, the precipitation in the Western Canadian Prairies is not strongly correlated with either. Bonsal and Lawford (1999) found that more extended dry spells tend to occur in the Canadian Prairies during the second summer following the mature stage of the El Nino events. The winter precipitation in Canada has a strong connection to ENSO (Shabbar *et al*. 1997), whereas summer precipitation, in most regions of western Canada (except the coast of British Columbia and Southern

294 Alberta), does not have a significant correlation with ENSO. This is consistent with our investigation
295 using instrumental records from 1948 to 2016.

296 Growing season precipitation in the Canadian Prairies is affected by many factors. Precipitation
297 deficits can occur under various circulation and lower boundary conditions. Thus, it is not expected that
298 a universal condition for all the significant droughts in the region can be identified. In fact, extreme
299 drought events have been found in both El Nino and La Nina years. A previous study by Bonsal and
300 Lawford (1999) indicates the meteorological drought often occurs after the mature phase of El Nino,
301 which is not the case for 2015. The associated anomaly in the North Pacific represented by NPM
302 positive phase is consistent with their results. The direct linkage between ENSO and the summer
303 precipitation in the Canadian Prairies is not clear. In fact, the correlation between MEI and the
304 precipitation in the investigated region is -0.096 ($p=0.239$, sample size = 152). The investigated region's
305 growing season precipitation does not possess a significant correlation with ENSO, which is consistent
306 with other researchers' findings (Dai and Wigley 2000).

307 The regression pattern is consistent with stationary Rossby wave theory as shown in a hierarchy
308 of theoretical and modelling studies (Karoly *et al.* 1989, Simmons *et al.* 1983, Hoskins and Ambrizzi
309 1993, Ambrizzi and Hoskins 1997, Held *et al.* 2002). A similar wave train extends from the western
310 Pacific toward extra-tropical South America but at lower latitudes compared to its counterpart in the
311 Northern Hemisphere (not shown). The node of the wave train in Western Canada and Northwest
312 Pacific of the US corresponds to an anomalous ridge, which is in-phase of El Nino forcing. When the
313 convection in the region associated with MJO-4 is weaker than normal (MJO-4 > 0), a wave train with
314 the opposite sign will reach western Canada which then counteracts the El Nino forcing. Thus, the weak
315 correlation between Canadian Prairie precipitation and ENSO is understandable as MJO plays an
316 additional role that enhances or cancels out the GPH anomaly caused by El Nino.

In the mid-latitude North America, the atmospheric response to the tropical forcing in the western Pacific depends on the mean circulation condition associated with tropical SST. Intraseasonal tropical convection oscillation in the western Pacific associated with the MJO-4 index cannot determine the sign of the precipitation anomaly in the Prairies alone. Both warm SST in central Pacific and strong tropical convection in western Pacific and Maritime Continent are essential to cause a significant precipitation deficit in the western Canadian Prairies. Warm SST in central Pacific causes an eastward expansion of Pacific warm pool that favours enhanced MJO activity in the western-central Pacific (Hendon *et al.* 1999, Marshall *et al.* 2016). As shown by the ray-tracing result, the NINO4 also affects the wavenumber of the quasi-stationary Rossby waves over the source region in the western Pacific. Under warm NINO4, the wavenumbers tend to be smaller due to stronger westerly in the source region and these waves can propagate northeastward into western Canada. Conversely, from May to August under cold NINO4, the westerly is weaker, and the meridional vorticity gradient is stronger in the subtropics near the source region. These mean flow conditions correspond to waves with lager wavenumbers that cannot propagate across the dateline.

In the year 2015, the SST anomaly in the Pacific (e.g. ENSO, NPM) coincided with the anomalous ridge on the west coast of Canada. This positive GPH anomaly was associated with the strong negative MJO4 indices, it then caused a blocking pattern and suppressed precipitation in the Canadian Prairies in the early summer through the mechanism discussed above. Although the El Nino continued to strengthen in July and August 2015, the active convection associated with MJO in the western Pacific propagated eastward into the central Pacific. As the convection in the western Pacific/Maritime Continent waned, the precipitation in the Canadian Prairie returned to slightly above normal in July.

# 5 Conclusions

The cause of the 2015 summer precipitation deficit in the western Canadian Prairies is investigated in relation to atmospheric circulation anomalies, SST, and intraseasonal tropical convection oscillation, MJO. The drought in western Canada is immediately related to an anomalous upper-level ridge that persisted over the west coast of Canada and Alaska since fall 2014. This ridge was likely associated with a developing El Nino that was enhanced by the MJO.

In general, MJO-4 indices demonstrated significant correlation with the meteorological drought over the Canadian Prairies from May to August when the SST in the central Pacific is warm (NINO4 > 0), which also corresponds to a stronger MJO amplitude in boreal summer. Our study discovered that MJO phase/strength is connected to the anomalous ridge over western Canada through the propagation of stationary Rossby waves from the western Pacific when NINO4 is positive. Though seasonally MJO is weaker in summer, the spring and early summer MJO amplitudes are larger than normal when the central Pacific SST is warmer than normal (NINO4 >0). The teleconnection between the Canadian Prairie precipitation deficit and MJO is stronger when NINO4 is positive. The underlying cause of this significant correlation between MJO-4 indices and the prairie precipitation in May-August is a stationary Rossby wave train originating from the Maritime Continent and western Pacific which propagates into Canada. The raytracing experiments show the main difference between a warm phase of NINO4 and a cold phase is the changes in stationary Rossby wave wavenumber over the source region. Under NINO4 > 0.5 May-August conditions, the total wavenumber is about 4 and can propagate into western Canada if they are oriented relatively zonally. Compared to NINO4 > 0.5, NINO4 < -0.5 corresponds to a weaker zonal wind and stronger meridional gradient of absolute vorticity in the subtropics of the source region (140°-150°E). Hence, the wavenumbers of stationary Rossby waves from the source region under NINO4 < -0.5 are larger (about 6), and these waves fail to reach the

Western Hemisphere. The intra-seasonal predictability of the growing season precipitation in the Canadian Prairies can be potentially improved by including the MJO amplitude and phase factors for medium-range/intra-seasonal projection in addition to ENSO effect especially when the central-Pacific SST is warm.

## Acknowledgment

We gratefully acknowledge the Natural Sciences and Engineering Research Council of Canada (NSERC) for funding the Changing Cold Regions Network (CCRN) through their Climate Change and Atmospheric Research (CCAR) Initiative. Dr. Zhenhua Li is supported by the Probing the Atmosphere of the High Arctic project sponsored by the NSERC. Dr. Yanping. Li gratefully acknowledges the support from the Global Institute of Water Security at the University of Saskatchewan. This research is also supported by Environment and Climate Change Canada (ECCC).

# References


Ambrizzi T and Hoskins B J 1997: Stationary Rossby-Wave Propagation in a Baroclinic Atmosphere, *Quart. J. Roy. Meteor. Soc.,* **123** 919–28.

Andrews, E.D., R.C. Antweiler, P.J. Neiman, and F.M. Ralph 2004: Influence of ENSO on Flood Frequency along the California Coast. *J. Climate,* **17**, 337–348, doi: 10.1175/1520-0442(2004)017.

Bonsal, B.R., Chakravarti, A.K. and Lawford, R.G. 1993: Teleconnections between North Pacific SST Anomalies and Growing Season Extended Dry Spells on the Canadian Prairies, Int. J. Climatol., 13, 865-878.

Bonsal, B.R., Zhang, X. and Hogg, W.D., 1999: Canadian Prairie growing season precipitation variability and associated atmospheric circulation, *Climate Research*, *11*(3), 191-208.

Bonsal B and Lawford R 1999: Teleconnections between El Niño and La Niña Events and Summer Extended Dry Spells on the Canadian Prairies, *International Journal of Climatology,* **19,** 1445–58.

Bonsal B R, Shabbar A and Higuchi K, 2001: Impacts of Low Frequency Variability Modes on Canadian Winter Temperature, *Int. J. Climatol.* **21,** 95–108.

Bonsal, B.R. and E. Wheaton, 2005: Atmospheric circulation comparisons between the 2001 and 2002 and the 1961 and 1988 Canadian Prairie droughts. Atmosphere-Ocean, 43 (2): 163–172.

Bonsal B R and Regier M, 2007: Historical Comparison of the 2001/2002 Drought in the Canadian Prairies, Climate Research, **33**, 229-242.

Bonsal, B R, Aider, R, Gachon, P and Lapp S, 2013: An Assessment of Canadian Prairie Drought: Past, Present, and Future, Climate Dynamics, **41**, 501–516.

Carbone R. E., Yanping Li, 2015: Tropical Oceanic Rainfall and Sea Surface Temperature Structure: Parsing Causation from Correlation in the MJO, *Journal of Atmospheric Science*, Vol. 72, No. 7, 2703–2718.

Cassou C, 2008: Intraseasonal Interaction Between the Madden-Julian Oscillation and the North Atlantic Oscillation, *Nature,* **455** 523–7.

Dai A and Wigley T M L, 2000: Global Patterns of ENSO-Induced Precipitation, *Geophys. Res. Lett.,* **27** 1283–6.

Dee D P, Uppala S M, Simmons A J, Berrisford P, Poli P, Kobayashi S, Andrae U, Balmaseda M A, Balsamo G, Bauer P, Bechtold P, Beljaars A C M, Berg L van de, Bidlot J, Bormann N, Delsol C, Dragani R, Fuentes M, Geer A J, Haimberger L, Healy S B, Hersbach H, Hólm E V, Isaksen L, Kållberg P, Köhler M, Matricardi M, McNally A P, Monge-Sanz B M, Morcrette J-J, Park B-K, Peubey C, Rosnay P de, Tavolato C, Thépaut J-N, and Vitart F, 2011: The ERA-Interim Reanalysis: Configuration and Performance of the Data Assimilation System, *Quarterly Journal of the Royal Meteorological Society,* **137,** 553–97.

Dey B, 1982: Nature and Possible Causes of Droughts on the Canadian Prairies-Case Studies, *Journal of Climatology,* **2,** 233–49.

425 Garfinkel C I, Feldstein S B, Waugh D W, Yoo C and Lee S, 2012: Observed Connection Between
426 Stratospheric Sudden Warmings and the Madden-Julian Oscillation, *Geophys. Res. Lett.,* **39.**
427
428 Hanesiak, J. M., Stewart, R. E., Bonsal, B. R., Harder, P., Lawford, R., Aider, R., *et al*. (2011).
429 Characterization and Summary of the 1999–2005 Canadian Prairie Drought. *Atmosphere-Ocean*, *49*(4),
430 421–452. http://doi.org/10.1080/07055900.2011.626757
431
432 Hartmann D L, 2015: Pacific Sea Surface Temperature and the Winter of 2014, *Geophys. Res. Lett.,* **42,**
433 1894–902.
434
435 Held I. M., Ting M. and Wang H., 2002: Northern Winter Stationary Waves: Theory and Modeling *J.*
436 *Climate,* **15**, 2125–44.
437
438 Hendon, H. H., C. Zhang, and J. D. Glick, 1999: Interannual variation of the Madden-Julian Oscillation
439 during Austral summer, J. Clim., 12, 2538–2550
440
441 Hong, C. C., Hsu, H. H., Tseng, W.-L., Lee, M. Y., Chow, C.-H., & Jiang, L.-C. 2017: Extratropical
442 Forcing Triggered the 2015 Madden–Julian Oscillation–El Niño Event. *Sci*. *Rep*. **7**, 46692; doi:
443 10.1038/srep46692.

444 Hoskins B J and Ambrizzi T, 1993: Rossby Wave Propagation on a Realistic Longitudinally Varying
445 Flow. *J. Atmos. Sci.* **50** 1661–71

446 Hoskins, B.J. and D.J. Karoly, 1981: The Steady Linear Response of a Spherical Atmosphere to
447 Thermal and Orographic Forcing. *J. Atmos. Sci.,* **38**, 1179–1196

448 Hoskins, B.J. and T. Ambrizzi, 1993: Rossby Wave Propagation on a Realistic Longitudinally Varying
449 Flow. J. Atmos. Sci., 50, 1661–1671
450
451 Huang B, Banzon V F, Freeman E, Lawrimore J, Liu W, Peterson T C, Smith T M, Thorne P W,
452 Woodruff S D and Zhang H-M, 2015: Extended Reconstructed Sea Surface Temperature Version 4
453 (ERSST. v4). Part I: Upgrades and Intercomparisons *Journal of Climate,* **28** ,911–30.

454 Kalnay E, Kanamitsu M, Kistler R, Collins W, Deaven D, Gandin L, Iredell M, Saha S, White G,
455 Woollen J, Zhu Y, Chelliah M, Ebisuzaki W, Higgins W, Janowiak J, Mo K, Ropelewski C, Wang J,
456 Leetmaa A, Reynolds R, Jenne R and Joseph D, 1996: The NCEP/NCAR 40-Year Reanalysis Project
457 *Bull. Amer. Meteor. Soc.* **77** 437–71
458
459 Karoly D J, Plumb R A, and Ting M, 1989: Examples of the Horizontal Propagation of Quasi-Stationary
460 Waves. *J. Atmos. Sci.* **46** 2802–11
461
462 Lee M Y, Hong C C and Hsu H H 2015: Compounding Effects of Warm Sea Surface Temperature and
463 Reduced Sea Ice on the Extreme Circulation Over the Extratropical North Pacific and North America
464 During the 20132014 Boreal winter *Geophys. Res. Lett.,* **42**, 1612–8.
465
466 Li Y., Richard E. Carbone, 2012: Excitation of rainfall over the tropical western Pacific. *Journal of*
467 *Atmospheric Science,* Vol. 69, No. 10, 2983–2994.
468
469 Li Y., Kit Szeto, Ron Stewart, Julie Theriault, Liang Chen, Bob Kochtubajda, Anthony Liu, Sudesh
470 Boodoo, Ron Goodson, Curtis Mooney, Sopan Kurkute, 2017: The June 2013 Alberta Catastrophic

Flooding: Water vapor transport analysis by WRF simulation. *Journal of Hydrometeorology,* Vol. 18, 2057-2078.

Li Z., Alan Manson, Yanping Li, Chris Meek, 2017: Circulation Characteristics of Persistent Cold Spells in Central-Eastern North America. *Journal of Met. Res*., Vol. 31, 250-260.

Liu J, Stewart R E and Szeto K K, 2004: Moisture Transport and Other Hydrometeorological Features Associated With the Severe 2000/01 Drought Over the Western and Central Canadian Prairies *Journal Of Climate,* **17**, 305–19.

Liu A., C. Mooney, K. Szeto, J. M. Thériault, B. Kochtubajda, R.E. Stewart, S. Boodoo, R. Goodson, Y. Li, J. Pomeroy, 2016: The June 2013 Alberta Catastrophic Flooding Event: Part 1 – Large scale features. *Hydrological Process*, 2016, 30*,* 4899–4916

Lorenz, D.J. and D.L. Hartmann, 2006: The Effect of the MJO on the North American Monsoon. *J. Climate,* **19**, 333–343, doi: 10.1175/JCLI3684.1.

Madden R A and Julian P R, 1971: Detection of a 40-50 Day Oscillation in the Zonal Wind in the Tropical Pacific, *J. Atmos. Sci.,* **28**, 702–8

Marshall, A. G., H. H. Hendon, and G. Wang, 2016: On the role of anomalous ocean surface temperatures for promoting the record Madden-Julian Oscillation in March 2015, Geophys. Res. Lett., 43,472–481.

493 Riddle E E, Stoner M B, Johnson N C, L'Heureux M L, Collins D C and Feldstein S B, 2013: The
494 Impact of the MJO on Clusters of Wintertime Circulation Anomalies Over the North American region
495 *Climate Dynamics,* **40**, 1749–66.
496
497 Rodney, M., Lin, H., & Derome, J. 2013: Subseasonal Prediction of Wintertime North American
498 Surface Air Temperature during Strong MJO Events. *Monthly Weather Review*, *141*(8), 2897–2909.
499 http://doi.org/10.1175/MWR-D-12-00221.1.
500
501 Ropelewski C F and Halpert M S 1986: North American Precipitation and Temperature Patterns
502 Associated with the El Niño/Southern Oscillation (ENSO), *Monthly Weather Review*, **114**, 2352–62.
503
504 Shabbar, A., Bonsal, B. and Khandekar, M., 1997: Canadian precipitation patterns associated with the
505 Southern Oscillation. Journal of Climate 10:3016-3027.
506
507 Shabbar A and Skinner W, 2004: Summer Drought Patterns in Canada and the Relationship to Global
508 Sea Surface Temperatures, *Journal of Climate,* **17**, 2866–80.
509
510 Shabbar A, Bonsal B R and Szeto K, 2011: Atmospheric and Oceanic Variability Associated with
511 Growing Season Droughts and Pluvials on the Canadian Prairies, *Atmosphere-Ocean,* **49**, 339–55.
512
513 Simmons A J, Wallace J M and Branstator G W, 1983: Barotropic Wave Propagation and Instability,
514 and Atmospheric Teleconnection Patterns, *J. Atmos. Sci.,* **40**, 1363–92.
515
516

Szeto, K., X. Zhang, R.E. White, and J. Brimelow, 2016: The 2015 Extreme Drought in Western Canada. *Bull. Amer. Meteor. Soc.,* **97**, S42–S46,https://doi.org/10.1175/BAMS-D-16-0147.1.

Wang S Y, Hipps L, Gillies R R and Yoon J-H, 2014: Probable Causes of the Abnormal Ridge Accompanying the 2013-2014, California Drought: ENSO Precursor and Anthropogenic Warming footprint *Geophys. Res. Lett.,* **41** 3220–6.

Xie P and Arkin P A, 1997: Global Precipitation: A 17-year Monthly Analysis Based on Gauge Observations, Satellite Estimates, and Numerical Model Outputs. *Bulletin of the American Meteorological Society,* **78,** 2539–58.

Xue Y, Higgins W and Kousky V 2002: Influences of the Madden-Julian Oscillations on Temperature and Precipitation in North America during ENSO-neutral and Weak ENSO Winters, *Proc. workshop on prospects for improved forecasts of weather and short-term climate variability on subseasonal (2 week to 2 month) time scales.*

Wheaton, E, Wittrock V, Kulshreshtha S, Koshida G, Grant C, Chipanshi A, Bonsal BR, 2005: Lessons Learned from the Drought Years of 2001 and 2002: Synthesis Report. Agriculture and Agri-Food Canada, Saskatchewan Research Council Publ No. 11602–46E03, Saskatoon.

Wheeler, M. C., & Hendon, H. H., 2004: An all-season real-time multivariate MJO index: Development of an index for monitoring and prediction. *Monthly Weather Review*, *132*(8), 1917–1932.

Wolter, K., 1987: The Southern Oscillation in surface circulation and climate over the tropical Atlantic, Eastern Pacific, and Indian Oceans as captured by cluster analysis. J. Climate Appl. Meteor., 26, 540-558.

Wolter, K. and M.S. Timlin, 1993: Monitoring ENSO in COADS with a seasonally adjusted principal component index. Proc. of the 17th Climate Diagnostics Workshop, Norman, OK, NOAA/NMC/CAC, NSSL, Oklahoma Clim. Survey, CIMMS and the School of Meteor., Univ. of Oklahoma, 52-57.

Zhang C, 2005: Madden-Julian Oscillation *Reviews of Geophysics,* **43.**

553

554 Table 1 Correlation between mean precipitation anomaly in the Prairies from CMAP and MEI, MJO

555 indices 4. MJO indices and CMAP are from 1979 to 2016.

| | Correlation | p-value | No. of sample |
|---|---|---|---|
| MEI | -0.096 | 0.24 | 156 |
| MJO-4 | 0.18 | 0.023 | 156 |
| MJO-4(NINO4>0) | 0.33 | 0.0015 | 90 |
| MJO-4(NINO4<0) | -0.01 | 0.94 | 66 |

556

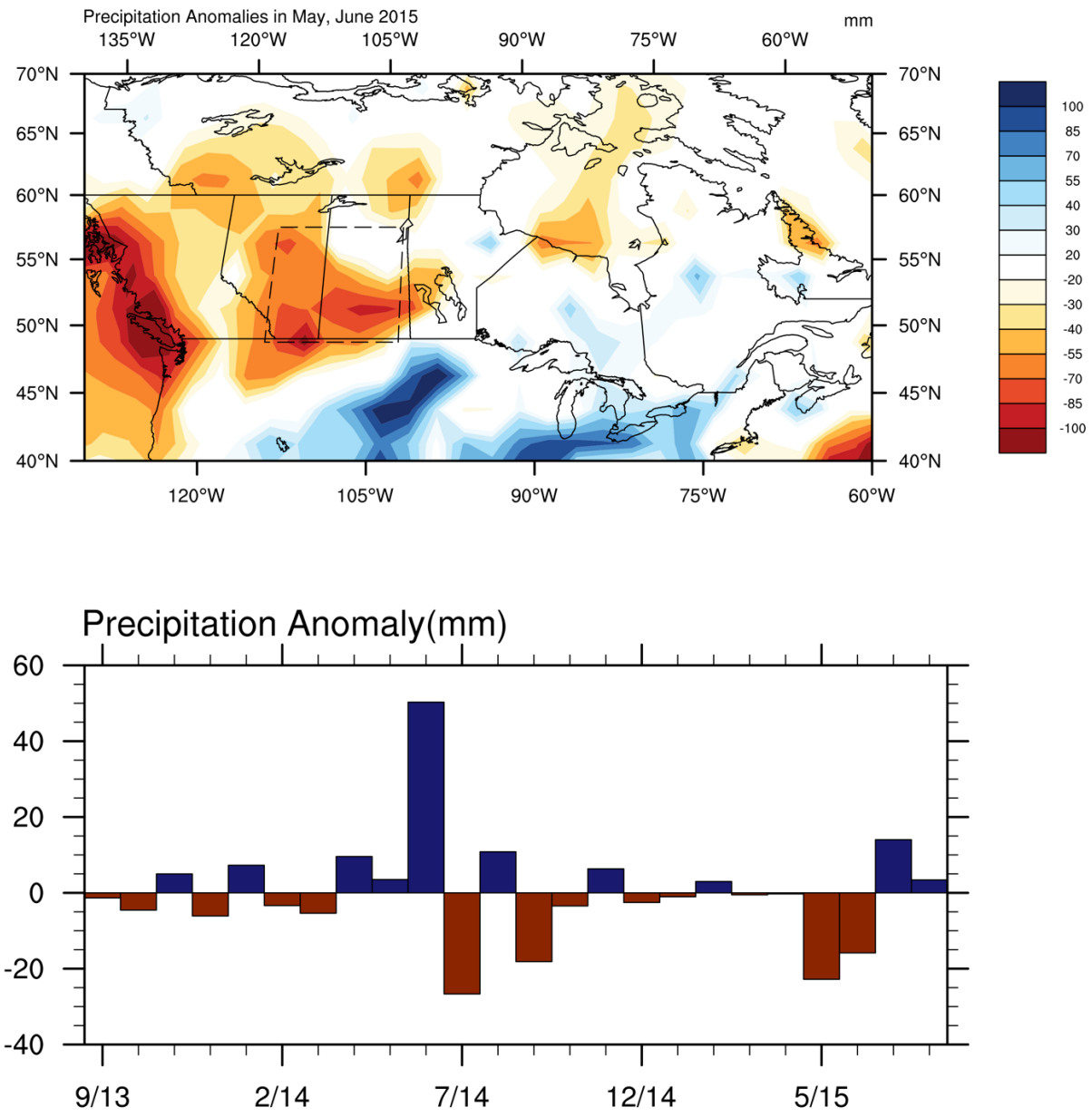


Fig. 1 Top: Precipitation anomalies (mm) from CMAP over the region (115 W-102.5 W, 50 N-57.5 N) during May and June 2015. Bottom: time series of monthly precipitation anomaly over boxed region between September 2013 and August 2015.

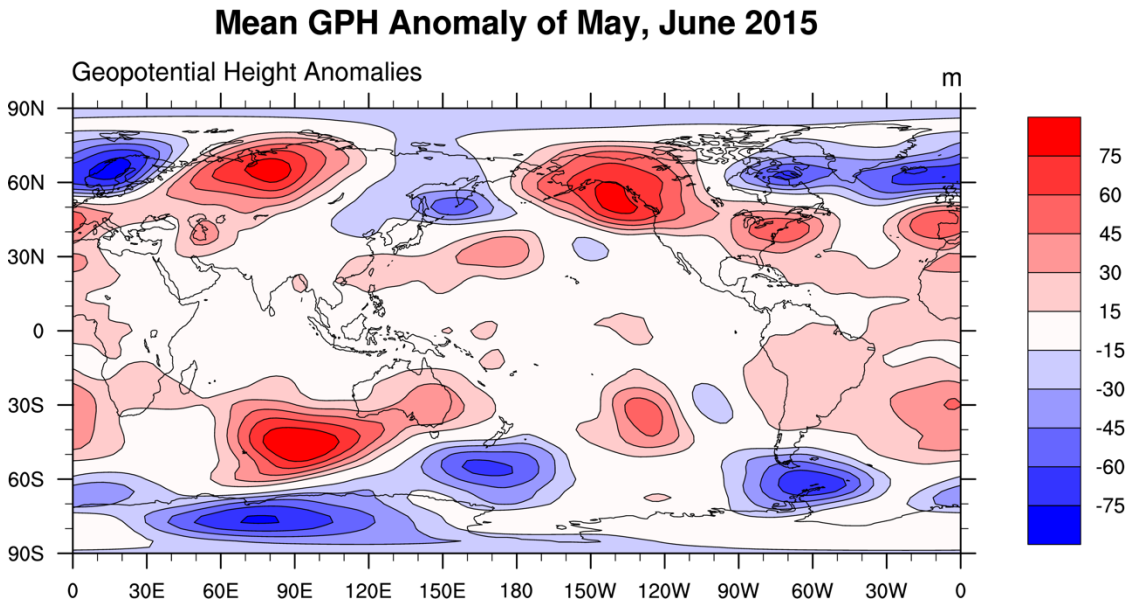


Fig. 2 NCEP GPH anomaly at 500hPa during May and June 2015 when the precipitation deficit was the largest.

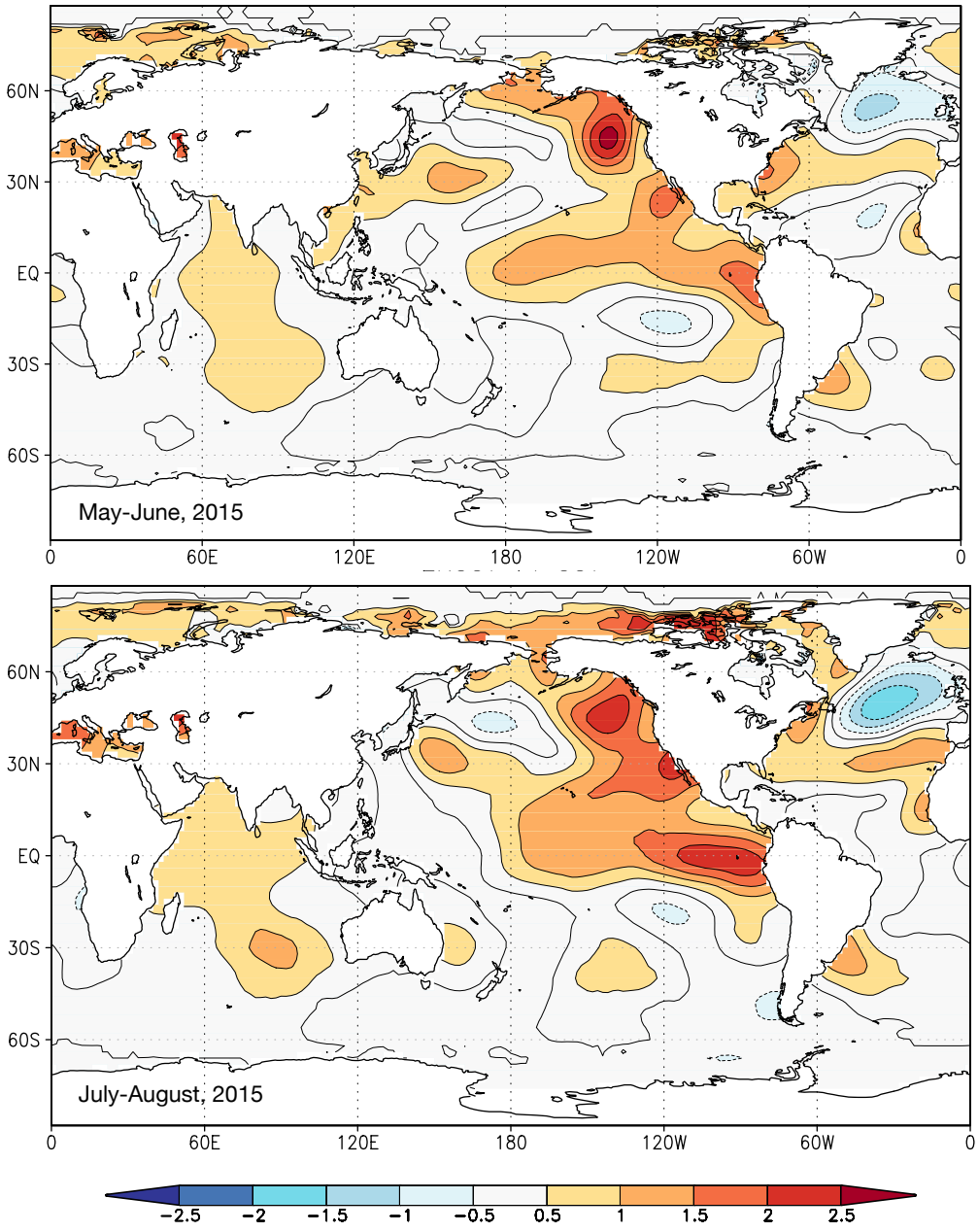


579

580 Fig. 3 The mean SST anomaly (ºC) from ERSST v4 for May-June and July-August 2015.

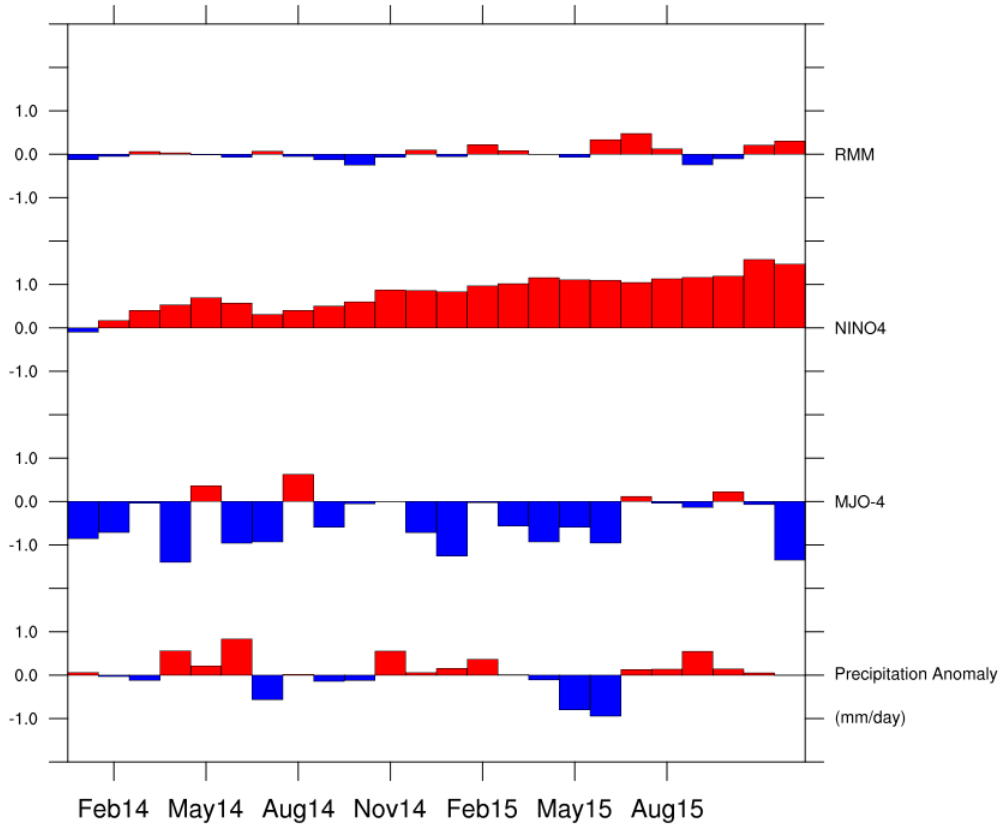


581

582 Fig. 4 RMM amplitude anomaly, NINO4, MJO 4 indices and precipitation anomaly of the Canadian

583 Prairies from January 2014 to Dec 2015.

584

585

586

587

588

589

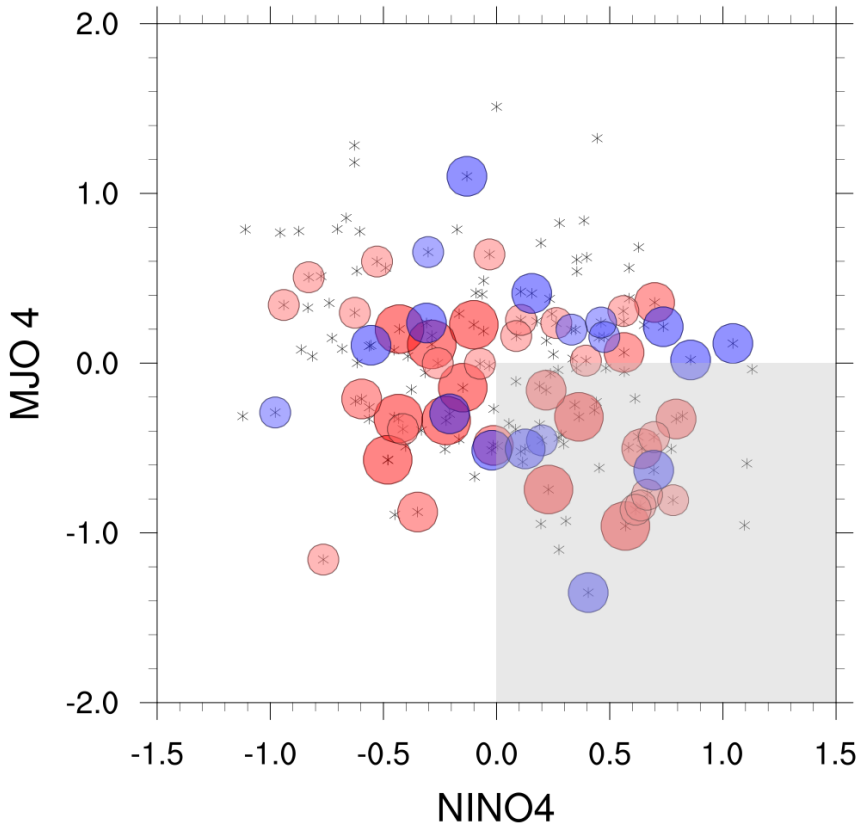


590

591 Fig. 5 The scatter plot of monthly precipitation anomaly (mm/month) as a function of MJO-4 and
592 NINO4. Each asterisk represents a month from May to August 1979-2016. Circled asterisk denotes a
593 month with precipitation anomaly larger than 18 mm/month. The blue circles are months with positive
594 precipitation anomaly and the red circles are months with negative precipitation anomaly. The sizes of
595 circles denote the magnitudes of the anomalies (large > 30 mm/month, medium > 24 mm/month,
596 small >18 mm/month). The shaded area denotes NINO4 > 0 and MJO-4 index < 0.

597

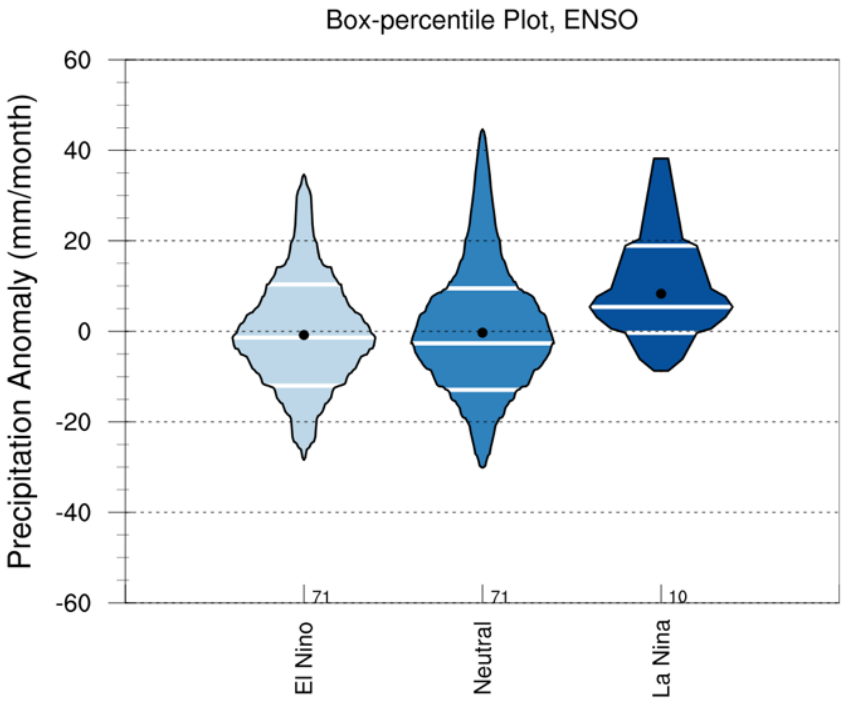


598

599 Fig. 6 The box-percentile plot of the Canadian Prairies precipitation anomaly during growing season

600 under different ENSO conditions.

601

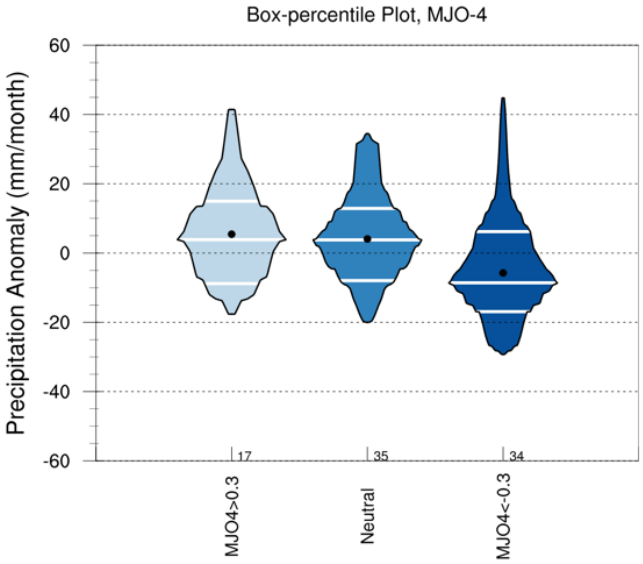


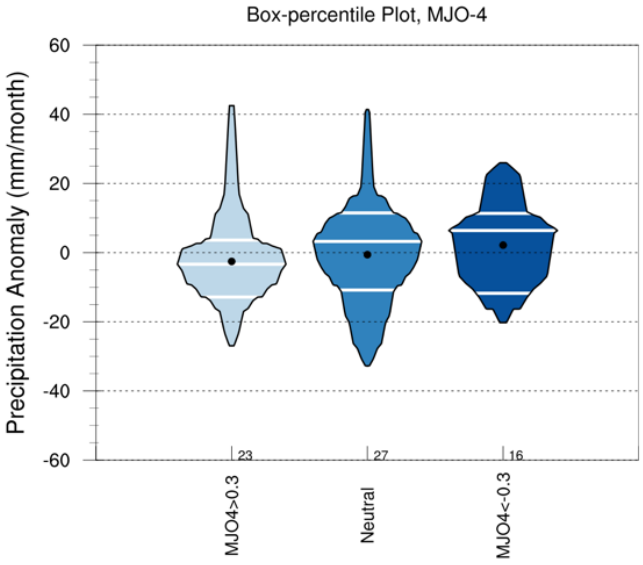


Fig. 7 Box-percentile plots of the Canadian Prairies' precipitation anomaly during growing season versus MJO-4 under warm NINO4 (NINO4> 0, top) and cold NINO4 (NINO4<0, bottom) SST condition.

610

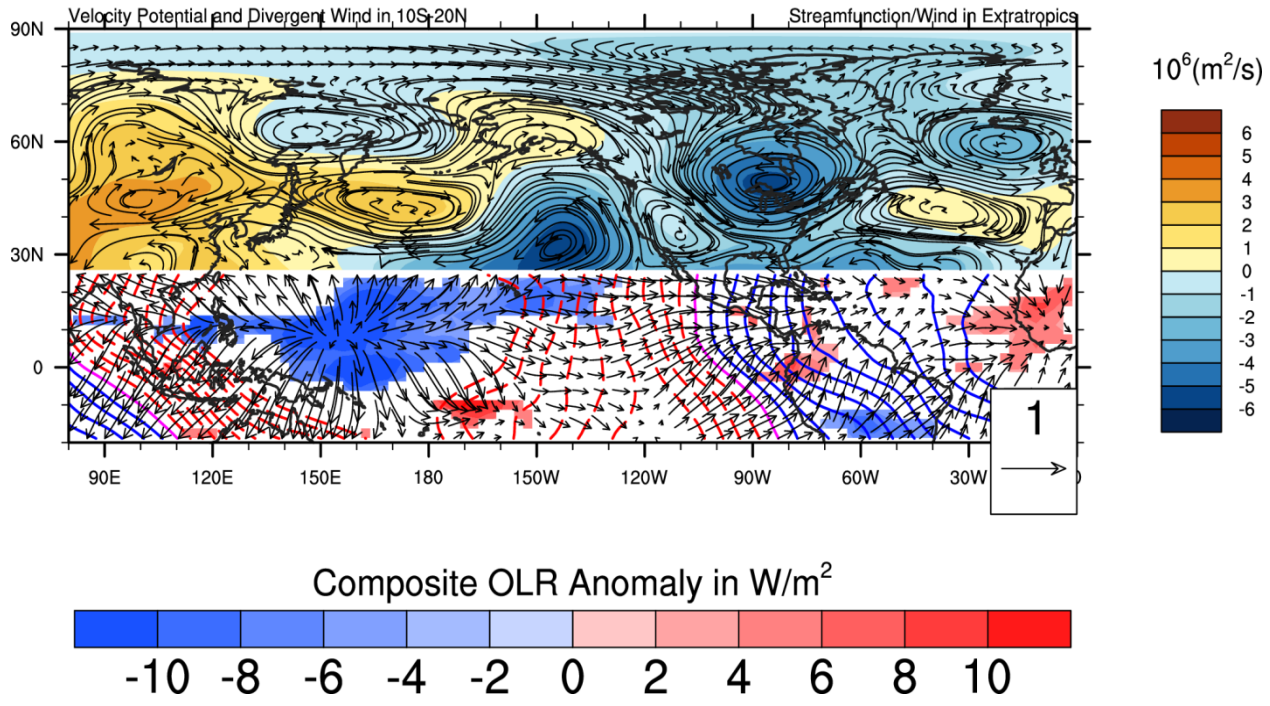


611

612

613 Fig. 8 The regression of stream function, wind field in the extratropics on negative MJO-4 for May-
614 August with NINO4 > 0.5 condition. In the tropics, the regression of OLR, velocity potential, and
615 divergent wind on negative MJO-4 indices for May-August with NINO4 > 0.5 condition. The shaded
616 region for the tropical OLR has p-value < 0.05. Blue shading indicates active convection region. Red
617 dashed contour and solid blue contour corresponds to negative and positive velocity potential,
618 respectively.

619

620

621

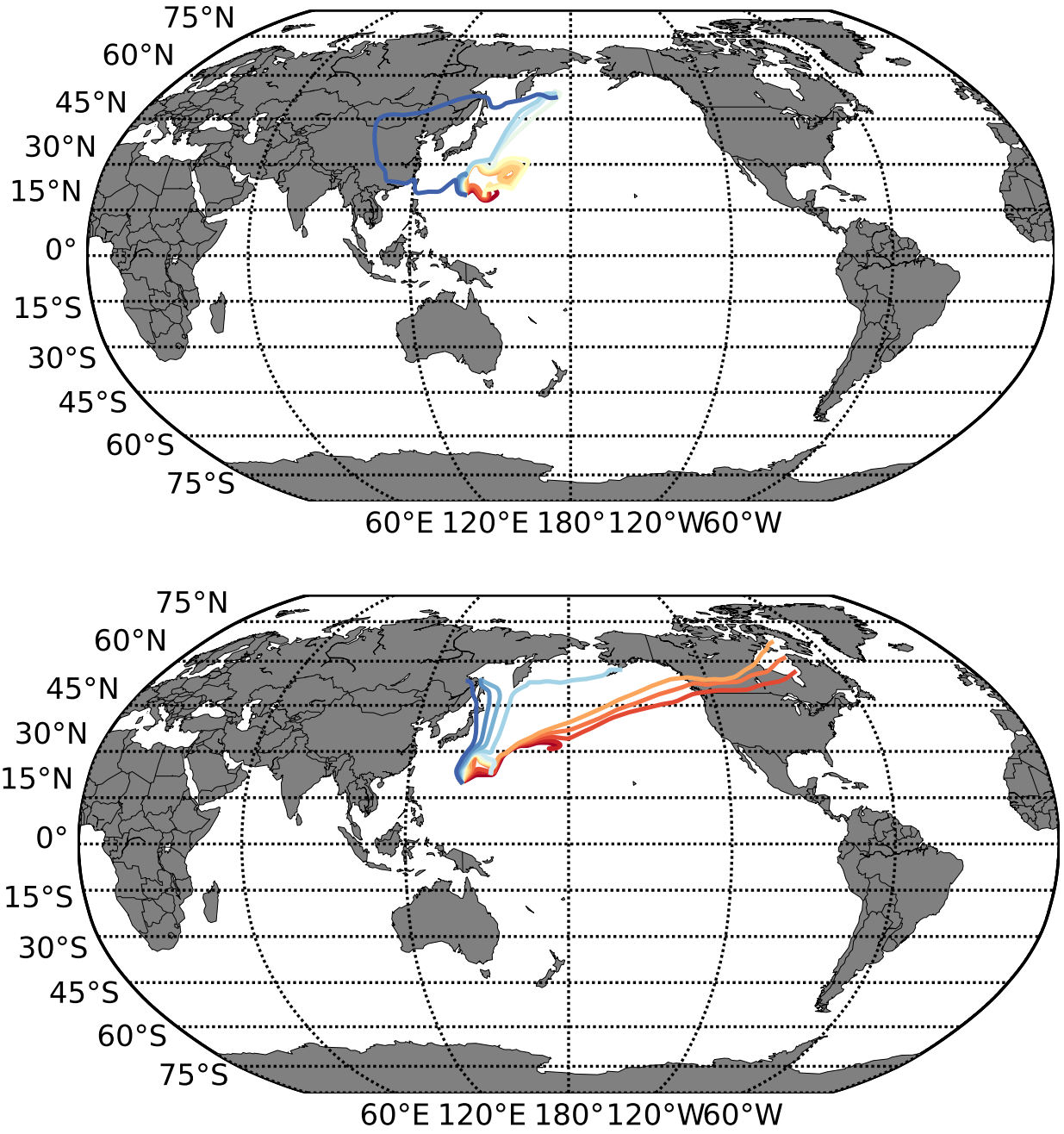


*Fig. 9: Ray-tracing result with total wavenumber specified by the mean flow 140-150W and 20-30N for mean May-August condition with NINO4<-0.5 (top) and NINO4>0.5 (bottom). Rays originate from 140E, 20N with angles ranging from 0 (red) to 60 degrees (dark blue) from zonal direction.*